

Role of homogeneous distribution of SiC reinforcement on the characteristics of stir casted Al–SiC composites

M.Saravana Kumar^{1,*}, S.Rashia Begum², C.I.Pruncu^{3,4}, Mehdi Shahedi Asl⁵,

^{1*} Department of Mechanical Engineering, Mount Zion College of Engineering and Technology, Pudukkottai, Tamil Nadu, India

² Assistant Professor, Department of Mechanical Engineering, College Of Engineering, Anna University, Chennai, Tamil Nadu, India.

³ Design, Manufacturing & Engineering Management, University of Strathclyde, Glasgow, G1 1XJ, Scotland, UK.

⁴ Department of Mechanical Engineering, Imperial College London, Exhibition Rd., SW7 2AZ, London, UK

⁵ Department of Mechanical Engineering, University of Mohaghegh Ardabili, Ardabil, Iran

*Corresponding authors: saravana312@gmail.com

Abstract

Stir casting process is very popular for the fabrication of particle reinforced metal matrix composites. However, achieving a homogenous distribution of the reinforcement particles is very challenging, which directly affect the final mechanical performances. In this research, a detailed investigation was conducted to obtain a superior synthesis of Al–SiC composite materials and to detect the effect of SiC particles distribution on the mechanical characteristic of the stir casted Al matrix composites using glycerol–water based model. The glycerol–water based model study displays the impacts of viscosity of Al melt (1.04-1.24 mPa.s), impeller position (10-50%), stirring speed (100-300 rpm) and blade angle (0-90°) on the vortex height, dispersion time, settling time and clustering of particles. The results of the experiments using glycerol–water based model, 45 ° blade angles, impeller position of 40% from the base, stirring speed of 250 rpm showed the best uniform distribution of reinforcement particles. Confirmation experiments were carried out by fabricating Al-SiC PRMMC based on three different viscosities (1.04, 1.13, and 1.24 mPa.s) of Al melt and considering other parameters as constant. Fabricated Al-SiC samples were analysed by Scanning Electron Microscope (SEM) and mechanical testing such as tensile, hardness and wear tests. Based on the confirmation results, the viscosity of 1.13 mPa.s for Al melt (at 750 °C) resulted in uniform distribution of SiC particles, which enhanced the tensile strength by 4%, wear resistance by 21%, and led to a uniform hardness value of 47 VHN throughout the composites.

KEYWORDS: Vortex flow; settling time; dispersion time; particle distribution; homogeneity.

1. Introduction

Aluminium based Metal Matrix Composites (MMCs) show an astounding mix of high specific strength and solidness, high wear resistance, great seizure resistance, improved fatigue and creep qualities [1-3]. Thus, impressive attention has been given for the investigation of the likelihood of utilizing materials of this class in vehicles, aerospace, military and other engineering applications [3-5].

1 Particle reinforced metal matrix composites can be manufactured by various procedures
2 including liquid, solid and vapour state routes [5-8]. Among these, liquid metallurgy has been
3 utilized for the fabrication of the most practical and economical parts [9]. Stir casting, a
4 liquid metallurgy technique, comprises of energetic blending of a liquid matrix by the use of
5 mechanical or magneto-hydrodynamic methods, followed by the introduction of
6 reinforcement into the liquid matrix [10]. Mostly, the created vortex pulls the reinforcement
7 particles into the matrix. Accordingly, the gas content of the slurry is additionally dependant
8 on blending parameters, such as stirrer blade angle and the speed of the impeller [11].
9

10 However, individual particles may form clusters at the vortex surface prior to their
11 entrance into the melt and may be transported to relatively stagnant zone where they survive
12 the shear forces of mixing and appear as clusters in the cast structure [12]. Inhomogeneity in
13 particle distribution in the cast composites can be overcome to a certain extent by
14 understanding the flow behaviour of reinforcements in liquid aluminium alloy melt at high
15 temperature during processing, analysing the flow behaviour at that high temperature is not
16 possible. However, a glycerol-water model can be used to clarify the behaviour of particles
17 in the molten metal.
18

19 Sandeep et al. [13] analysed six strategies to obtain uniform distribution of the
20 reinforcement particles. The strategies were implemented by varying the tool offset position.
21 They concluded that the groove method with tool offset gives enhanced homogenous
22 distribution of particle. Sharma et al. [14] used the optimization technique to analyse the
23 distribution index and the area fraction of composite. Stir casting parameters such as stirring
24 speed, furnace temperature and preheat temperature were also analysed using Response
25 Surface Methodology optimization. Subramani et al. [15] investigated the corrosion
26 behaviour and mechanical properties of the metal matrix composites by varying the
27 composition of the reinforcement particles i.e. Al_2O_3 , B_4C , and SiC particles. Corrosion tests
28 were carried out with the help of hydrochloric acid and sodium chloride solutions. The
29 outcome showed that the corrosion resistance and the mechanical properties were improved
30 by adding 4-5% reinforcement particles. Suthar et al. [16] listed out some issues such as
31 porosity, wettability, chemical reactions and particle distribution. These issues were
32 overcome by optimization of the stir casting parameters. Sahu et al. [17] used the grey
33 relation analysis to study the processing parameters such as friction factors, load and the
34 aspect ratio in the cold upsetting. The optimized parameter showed significant increase in the
35 quality characteristics. Dutta et al. [18] evaluated the stir casting process parameters for the
36 attainment of effective reinforcement particles. It was observed that the stirring time and
37 processing temperature have significant effects on the mechanical properties (elastic modulus
38 and hardness) and microstructure of the composites. Kumar et al. [19] analysed the mechanical
39 behaviour of the metal matrix composites by changing the composition of the reinforcements.
40 They observed that the 7.5wt% Al_2O_3 shows enhanced mechanical properties such as
41 hardness, tensile strength and toughness and also uniform distribution of the reinforcement
42 particles.
43

44 In this research, we have performed a systematic synthesis of Al-SiC composites
45 throughout which were able to obtain a uniform distribution of the reinforcement particles. It
46 leads to a significant improvement in overall strength of the manufactured composites. To
47 obtain the best SiC particles distribution we have investigated the influence of viscosity of Al
48 melt (1.04-1.24 mPa.s), impeller position (10-50%), stirring speed (100-300rpm) and blade
49 angle (0-90°) using glycerol-water based model. The uniform distribution of the SiC particles
50 in the Al matrix was proved by microstructural analysis and its role on the performance of the
51 stir casted samples was evaluated by mechanical testing procedures. The present research can
52 be used as a platform for creating superior parts for aerospace components due to the
53
54
55
56
57
58
59
60
61
62
63
64
65

robustness of the synthesis technique proposed which leads to superior mechanical properties of Al-SiC composites manufactured.

2. Materials and Methods

Real time stir casting setup for processing of SiC reinforced Al matrix composites was replaced with glycerol–water based experimental setup. The crucible was replaced with a transparent container of 35 mm radius and 90mm height for easily tracing of the particle distribution inside the container. The size and shape of this vessel were the same as those of the crucible used for the composite manufacturing. Agitation was provided by four bladed impellers with five different blade angles (0, 30, 45, 60 and 90⁰). The width and thickness of blades were kept constant for all the blade angles. Fig. 1(a) shows the schematic setup of the stirring vessel used in this study. Various stirrer speeds from 100 to 300rpm were offered by the variac controlled motor in which the impeller was attached. Glycerol–water mixture was chosen as the liquid medium for the simulation of the liquid aluminium behaviour considering its ease of handling and transparency. SiC particles (63 microns) were selected as the reinforcement material due to the non-reactive nature of silicon carbide. Impeller positions were adjusted from 10 to 50% from the base of the container. Based on the viscosity of the Al melt at five different working temperature (700, 726, 751, 776 and 800°C), five different glycerol–water based mixtures were prepared with the corresponding viscosity of Al melt. Details of the blending proportion of glycerol–water mixtures are tabulated in Table 1. The glycerol–water mixture behaves as a Newtonian fluid. A high resolution camera (CANON EOS 1300D) was used to capture the settling time, dispersion time, clustering of particles and vortex height.

Table 1. The blending proportion of glycerol and water.

Temperature of Al (°C)	Viscosity of Al (mPa.s)	Glycerol–water mixture		Viscosity of glycerol–water mixture. (mPa.s)
		Glycerine (ml)	Water (ml)	
700	1.24	0.014	0.186	1.25
730	1.18	0.010	0.190	1.17
750	1.13	0.008	0.192	1.13
780	1.08	0.005	0.195	1.08
800	1.04	0.003	0.197	1.05

The conditions embedded in the systematic experiments are approximately the same of that used for the Al-SiCp system, which are considered as standard parameters affecting the uniform distribution of the SiC particles. Further, the glycerol water mixture – SiC particle (1300Kg/m³ -3200Kg/m³) was chosen because its density is approximately the same of Al-SiCp (2300Kg/m³ -3200Kg/m³) synthesis. These density differences in glycerol water mixture – SiC particles (1300Kg/m³ -3200Kg/m³) were detected by quick observation of the distribution of SiC particles. As soon as the stirrer stops, particles were drawn from the specified location without giving any time for settling of particles.

A translucent plastic vessel was filled with a mixture of glycerol–water and SiC particles for enabling easy visual observation of the air entrapment, particle movement path, dispersion time, settling time, vortex height and clustering of particles in the stirred liquids [20]. In order

1 to find the clustering of the particles, samples were withdrawn from the mixture of glycerol–
2 water – 10 wt% SiC particles at specified locations, using a pipette fitted with a pump for
3 smooth and stable suction. The removed samples of SiC particles in the particular region of
4 the glycerol–water mixture were filtered using a filter paper to ensure all the SiC particles
5 were trapped in the filter paper and dried in an oven to remove the moisture and reweighed to
6 determine the amount of dried SiC particles. In order to obtain significant amount of SiC
7 particles at each time, very limited quantity of mixture (5 ml/suction) was taken without
8 creating any local disturbance. Four samples were taken at each sampling position and the
9 average weight was calculated for the estimation of SiC concentration at that location. A
10 camera was fixed along the same horizontal plane of the beaker. Shutter speed, aperture, and
11 lighting settings were adjusted for the optimization of the picture quality. Steady-state flow
12 patterns were arranged in the glycerol–water mixture with various stirring speeds. Before
13 stirring, the SiC particles were kept at the bottom of the glycerol–water mixture in the
14 container. After the stirring, the dispersion of the particles was recorded. Dispersion time is
15 defined as the time required for the reinforcement particle to distribute throughout the molten
16 matrix. The dispersion time depends upon various parameters such as stirrer geometry,
17 viscosity of Al melt, stirring speed and impeller position. As soon the stirring stopped, the
18 time taken for the settling time of the SiC particles was recorded. The settling time is defined
19 as the time required for the reinforcement particles to settle down at the bottom of the
20 container. This settling of reinforcement particles was mainly due to the density difference
21 between the molten matrix and the reinforcement. The influence of the different stirrer
22 height, viscosity, stirring speed and stirrer geometry over the vortex height (Fig. 1(a)) of the
23 stirrer liquid was also examined. Al-SiC composites were synthesised based on the effective
24 process parameters obtained from the systematic experiments using glycerol-water based
25 model. The manufactured specimens were evaluated for microstructural and mechanical
26 properties. In this research we conducted the microstructural evaluation using an advanced
27 optical tool which is the Scanning Electron Microscope (JEOL JSM-6380LA). It enables
28 magnifications ranging from 10X to 30,000X. The mechanical testing was carried out using
29 the tensile test and Vickers hardness test and wear test. The Tinius Olsen Computerized
30 Universal Testing Machine, H50KL model was used to find the tensile properties for the cast
31 specimens. Vickers micro-hardness tester was used to find the hardness value of the cast
32 specimens and the wear trials were conducted using the DUCOM pin-on-disc wear testing
33 apparatus.

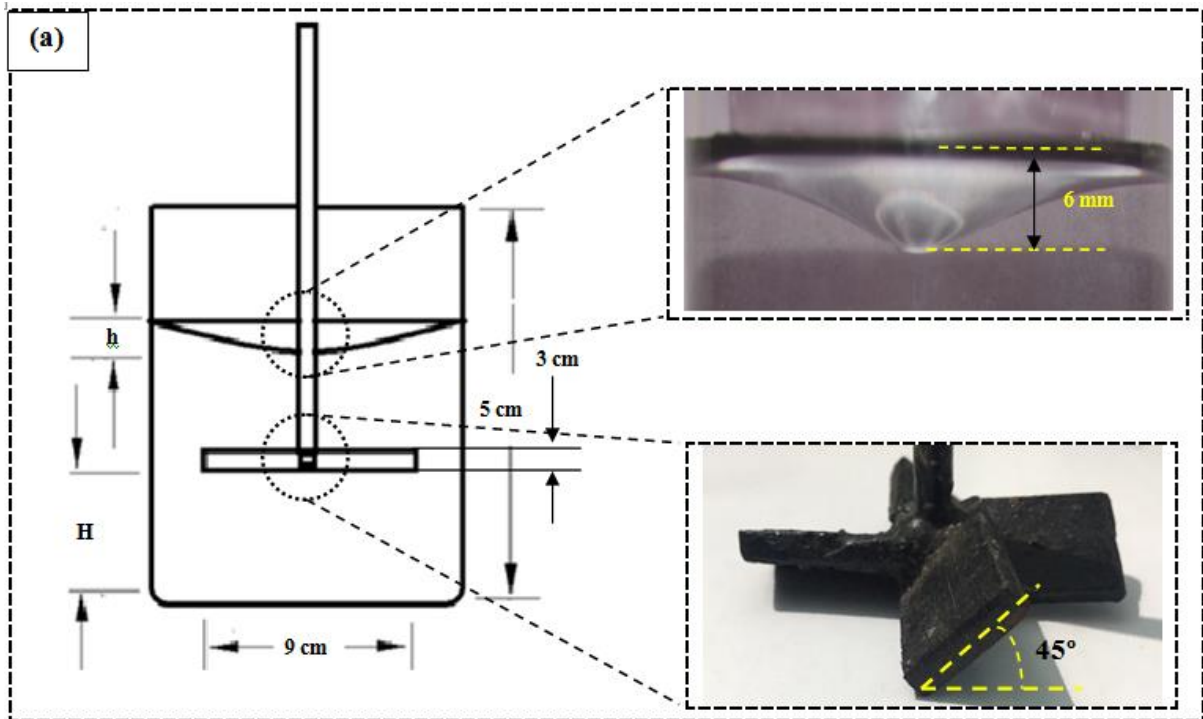
41 **3. Results and Discussion**

42 **3.1 Glycerol–water based experiments**

43 **3.1.1 Effect of viscosity**

44 The significant effects of the viscosity of the Al melts over the vortex height, dispersion time,
45 settling time and clustering of the particle are evident. Vortex height increases from 4 to 11
46 mm with decrease in the viscosity of the glycerol–water mixture from 1.24 to 1.04 mPa.s. A
47 decrease in viscosity is followed by an increase in vortex height leading to the air entrapment
48 and bubble formation. Later it formed porosity and void formation during solidification,
49 which can affect the mechanical properties. The disadvantage of increased viscosity is that it
50 increases the lack of fluidity. 85% of all particles settled before 60sec in glycerol–water
51 solution (Fig. 1(b)) and the complete settling is observed after 120sec (Fig. 1(c)). The settling
52 of SiC particles in the glycerol–water mixture after 60sec was evident from the appearance of
53 a clear layer showing the absence of SiC particles at the top of the mixture (Fig. 2).When the
54 viscosity of the glycerol–water mixture decreases, the dispersion time of the particle
55 decreases (Fig. 3(a))and also the settling time of the SiC particles decreases (Fig. 3(c)).The
56
57
58
59
60
61
62
63
64
65

1 settling time of the SiC particles was longer than the dispersion time of the particles, despite
2 the similarity in the order of magnitude. The setting time was independent of the impeller
3 speed and the blade angle, showing no variation but mainly dependent on fluid viscosity.
4 Soon after the stopping of the stirring within the fluid, the settling time began to occur [21].
5 Immediate solidification of the metal matrix composite materials was required for the
6 attainment of uniform distribution of the particles. Fig. 4 shows an increase in clustering at
7 the bottom with a decrease in the viscosity of the fluid. This was mainly due to the density
8 differences between the matrix and the reinforcement. The standard deviation values for the
9 percentage of SiC particles obtained from top, middle and bottom of the container with
10 respect to various viscosities were also mentioned in the Fig. 4. Due to the high density 3200
11 Kg/m³ of SiC particles will always tries to settle down, which led to the clustering of
12 particles. Clustering takes place at a lower viscosity at the bottom region of the fluid. At
13 higher viscosity, there was no uniform distribution of the particle because of the lack of
14 fluidity. The result showed the concentration of the SiC particles was higher in the lower
15 region at the lower viscosity of the fluid where there is no uniform distribution of the SiC
16 particles. Uniform dispersion of the SiC particles was obtained only at the viscosity of 1.13
17 mPa.s (Fig. 4) that is equal to the viscosity of molten aluminium at 750°C.



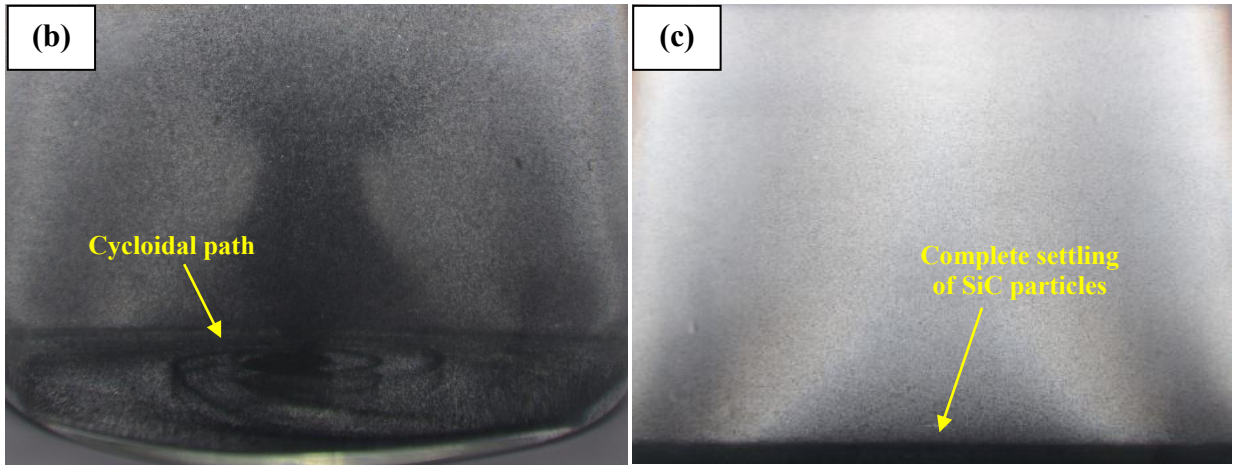


Fig. 1 (a) schematic setup of the stirring experiment with vortex height and 45° stirrer blade, (b) settling in cycloidal path and (c) complete settling of SiC particles.

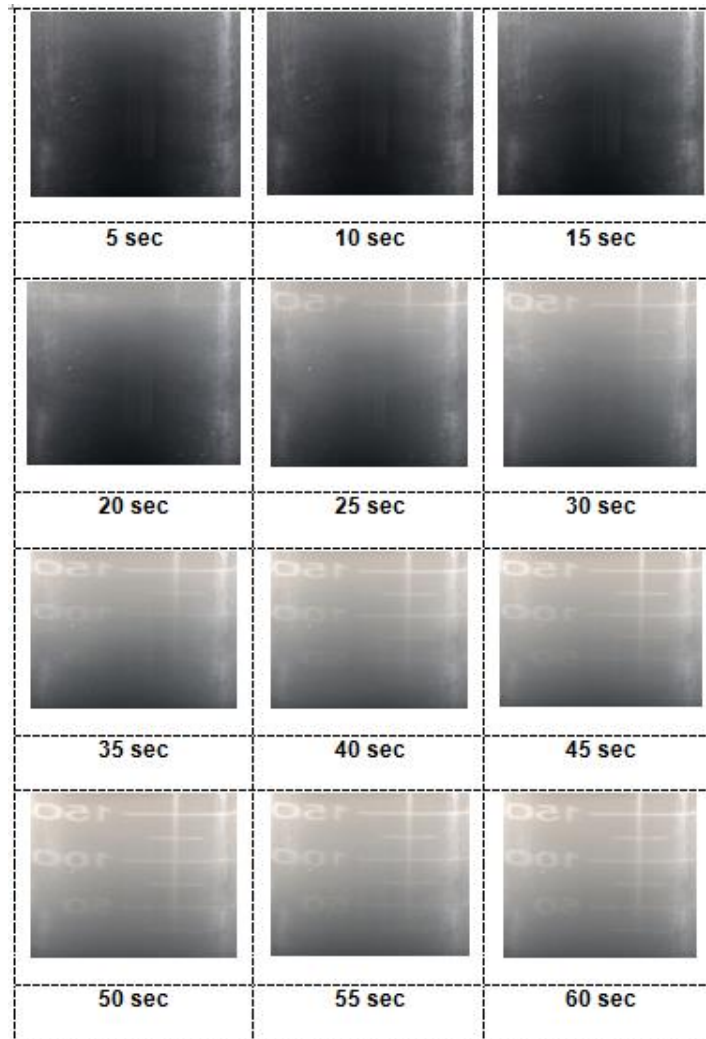


Fig. 2. Settling of SiC particles at various time intervals.

1
2
3
4
5
6
7
8
9
10
11
12
13
14
15
16
17
18
19
20
21
22
23
24
25
26
27
28
29
30
31
32
33
34
35
36
37
38
39
40
41
42
43
44
45
46
47
48
49
50
51
52
53
54
55
56
57
58
59
60
61
62
63
64
65

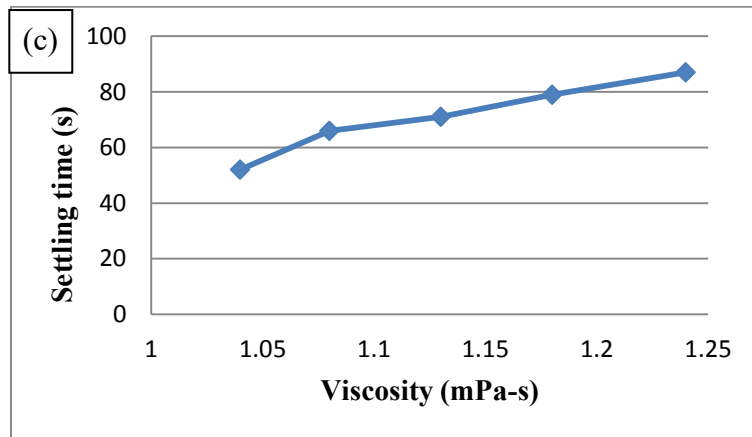
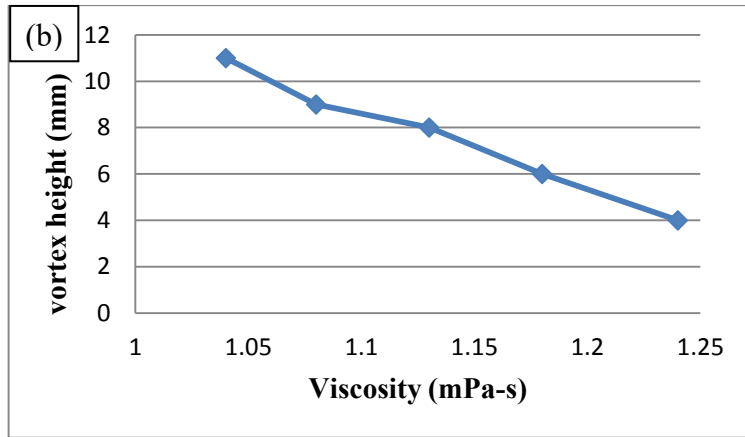
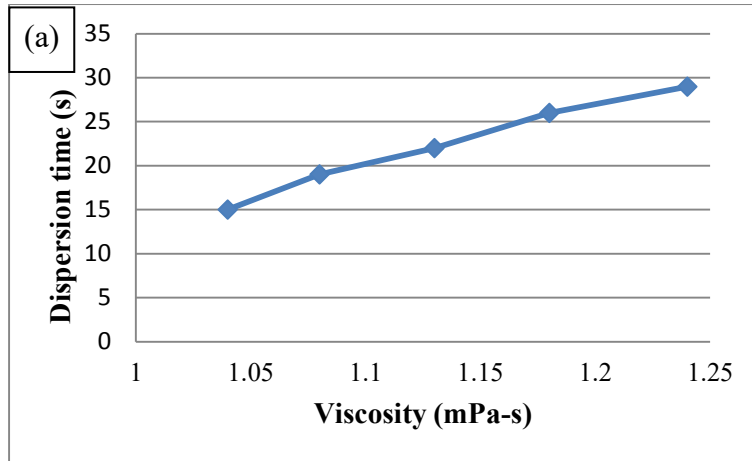


Fig. 3.(a) Viscosity vs. dispersion time, (b) viscosity vs. vortex height and (c) viscosity vs. settling time.

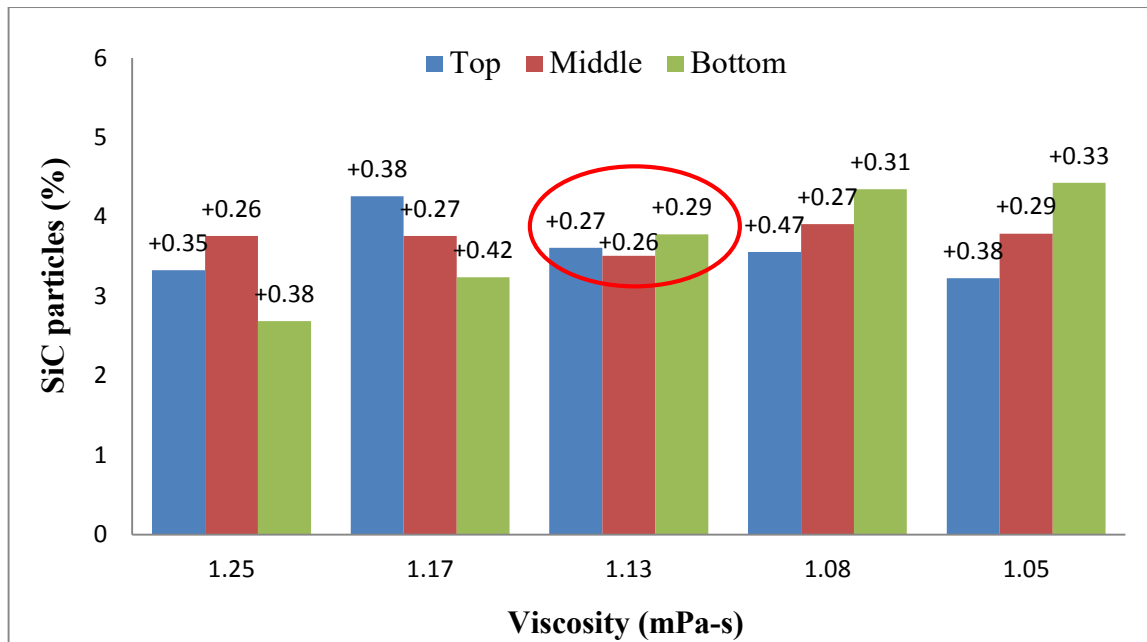


Fig. 4. Percentage of SiC particles obtained from top, middle and bottom of the container with respect to various viscosities of glycerol–water mixture.

3.1.2 Effect of blade angle

The blade angle has a significant effect over the dispersion time, vortex height and clustering of the particles. Increase in vortex height was seen with an increase in the blade angle (Fig. 5(a)). The increase in the blade angle not only caused an increase in the vortex height but also decreases the dispersion time (Fig. 5(b)). It was observed that at 0 and 30° blade angles lower vortex produces; therefore, there is no uniform dispersion of the particles. At 45 and 60° blade angles, uniform distribution of the particles and lower dispersion time were observed. Blade angle of 90° produced high vortex height, leading to air entrapment and affecting the uniform distribution of the particles. Despite higher blade angle producing a lower dispersion time, it did not produce uniform distribution of the particle. It is evident that the 90° blade angle leads to higher vortex pressure, which draws more particles and causes the agglomeration. For 45 and 60° blade angles, the distribution of SiC particles was uniform throughout the top, middle and bottom regions of the fluid (Fig. 6). When compared with 45 and 60° blade angles, 45° blade angles shows better uniform distribution of particles. While 0 and 30° blade angles did not create any sufficient pressure to distribute the particles, so the clustering was obtained at a lower region of the fluid. The standard deviation values for the percentage of SiC particles obtained from top, middle and bottom region of the container with respect to various blade angles were also mentioned in the Fig. 6. It was shown that the higher blade angle leads to a higher clustering of the particles, which affects the uniform distribution of them. Hence, 45° blade angles show better uniform distribution of particles when compared with all the blade angles and it was carried out for the confirmation experiments.

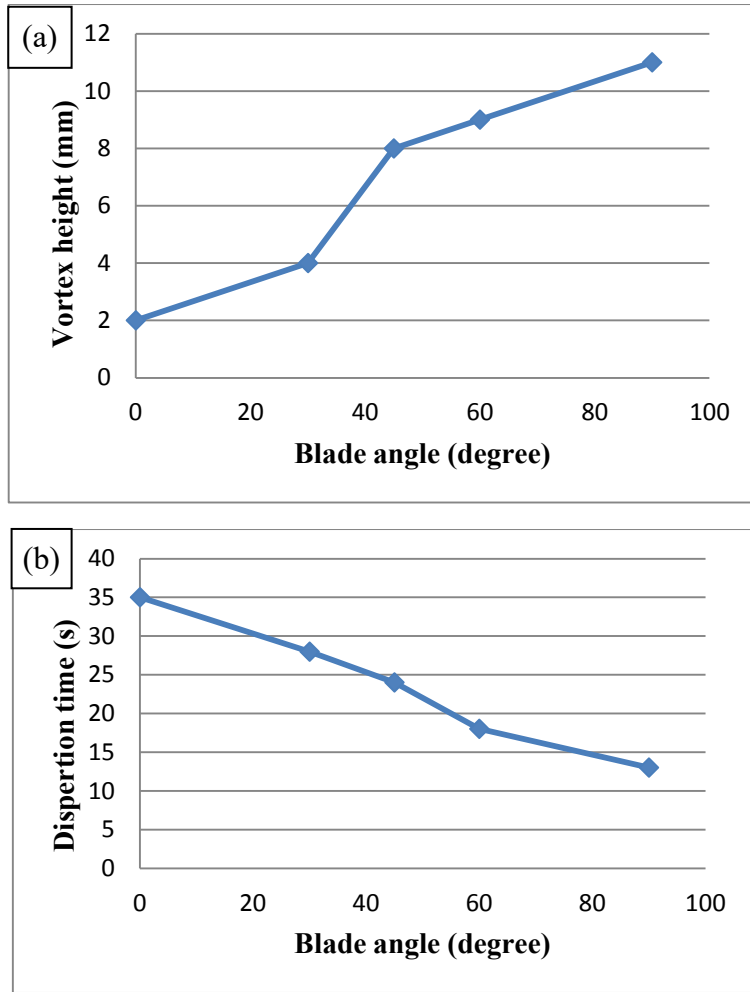


Fig. 5.(a) Blade angle vs. vortex height and (b) blade angle vs. dispersion time.

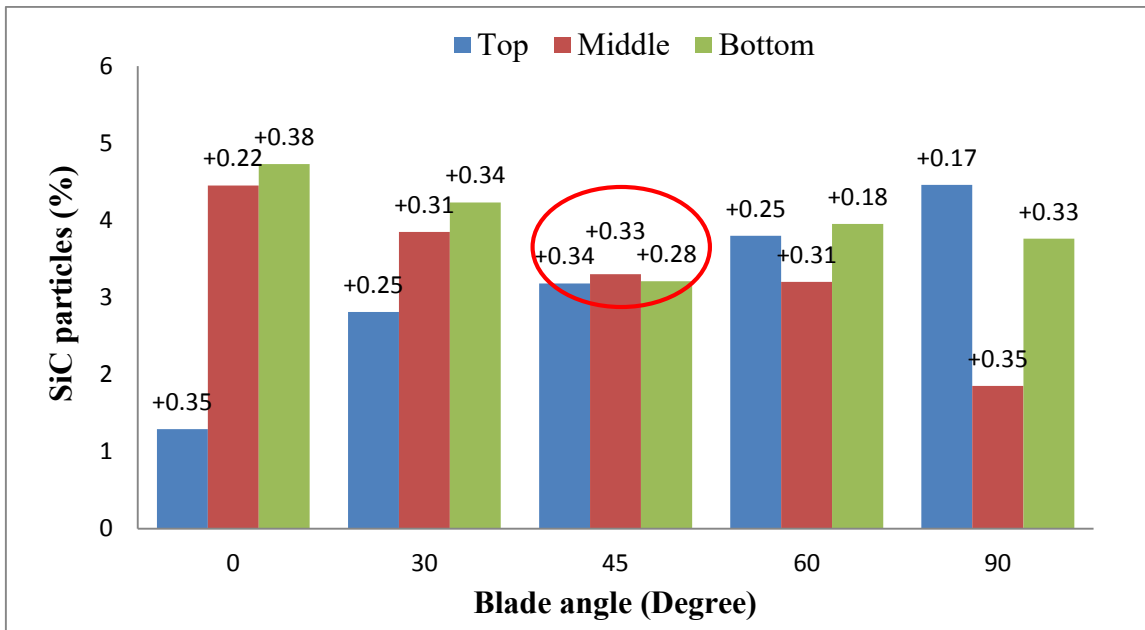


Fig. 6. Percentage of SiC particles obtained from top, middle and bottom of the container with respect to various stirrer blade angles.

3.1.3 Effect of stirring speed

The vortex height increases with increase in the stirring speed (Fig. 7(a)). At 100 and 150 rpm, there was no uniform distribution of the particles. Such low stirring speeds produced the lower vortex and increases the dispersion time. It was observed that the dispersion time decreases with an increase in the stirring speed (Fig. 7(b)). At 200 and 250 rpm, sufficient vortex pressure can be produced to distribute the particles in the fluid. A perfect vortex may be created without air entrapment and bubble formation. If the stirring speed goes beyond the 250 rpm, air entrapment takes place. A higher vortex was obtained by the higher stirring speed. At the 100 and 150 rpm stirring speeds, concentration of the SiC particles was more in the lower region of the fluid because of the inadequate vortex pressure. Uniform dispersion of SiC particles was obtained by 200 and 250 rpm stirring speeds as it provided sufficient vortex pressure to distribute all the particles uniformly over the top, middle and the bottom regions of the fluid. When compared with 200 and 250 rpm stirring speeds, 250 rpm stirring speed shows enhanced distribution of particles. For the high stirring speed, the dispersion time of reinforcement particles was very low due to the higher centrifugal force. The 300 rpm stirring will leads to higher shear rate which carries the particles to the top region of the fluid by centrifugal force which consequently led to an improper distribution of the SiC particles. The standard deviation values for the percentage of SiC particles obtained from top, middle and bottom region of the container with respect to various stirring speed were also mentioned in the Fig. 8. It is evident that the clustering increases by the higher stirring speeds because of the higher shear rate (Fig. 8). So, 250 rpm stirring speed was carried out for confirmation experiments.

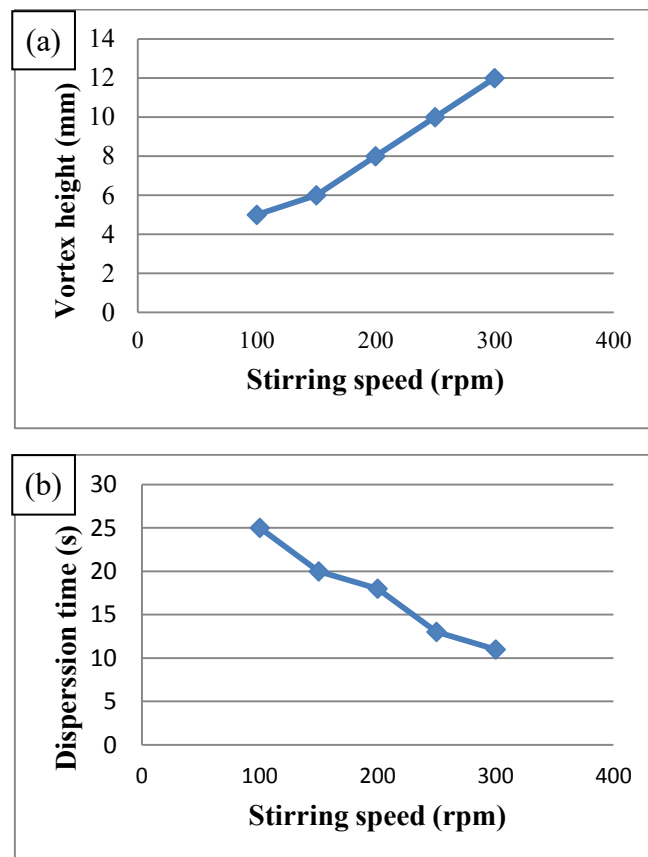


Fig. 7. (a) Stirring speed vs. vortex height and (b) stirring speed vs. dispersion time.

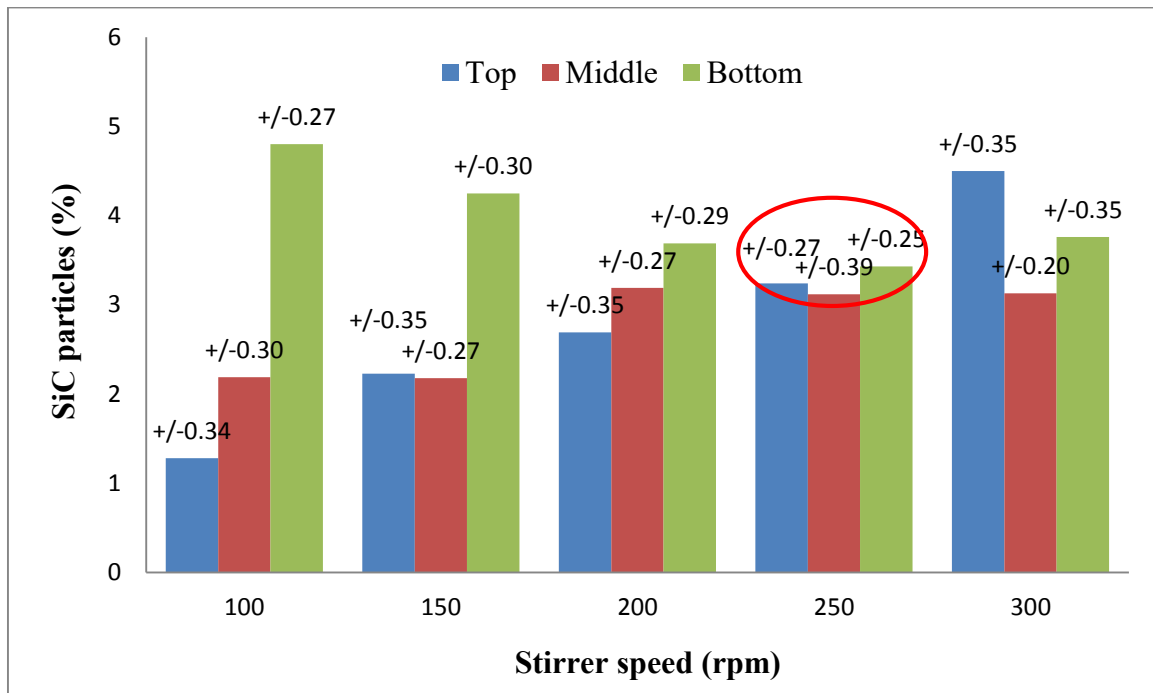


Fig. 8. Percentage of SiC particles obtained from top, middle and bottom of the container with respect to various stirring speed.

3.1.4 Effect of impeller position

It was observed that the vortex height decreases with an increase in the impeller position (Fig. 9(a)) and also an increase in the stirrer height in the fluid causes an increase in the dispersion time (Fig. 9(b)). The standard deviation values for the percentage of SiC particles obtained from top, middle and bottom region of the container with respect to various impeller positions were also mentioned in the Fig. 10. Stirring at the lower portion provides a better vortex and dispersion time compared to the stirring at the middle position. Stirring at the lower portion (10% from the base) of the fluid gave rise to more clustering at the top region of the fluid due to the higher vortex pressure at the bottom, which carried most of the SiC particles to the upper region (Fig. 10). Stirring at the middle position (50% from the base) also gave rise to a larger agglomeration of particles at the bottom of the fluid because at the bottom no vortex pressure is created. Most of the particles formed clusters at the base of the fluid due to the low vortex pressure. Hence, the stirrer was placed at the 40% from the base in order to produce particle entrapment and to prevent air entrapment. So, impeller position of 40% from the base was carried out for confirmation experiments.

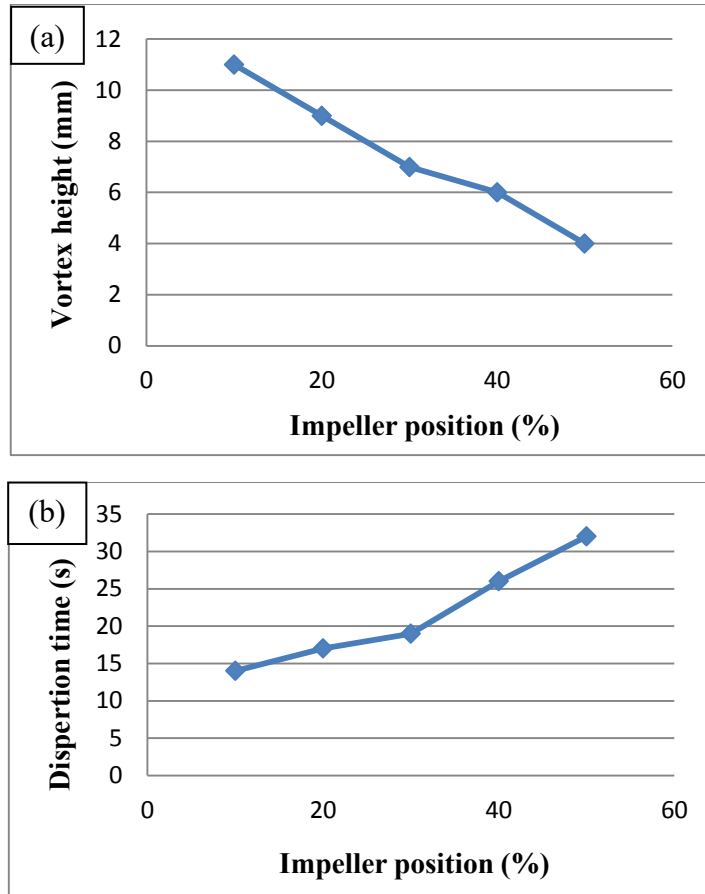


Fig. 9.(a) Impeller position vs. vortex height and (b) vs. dispersion time.

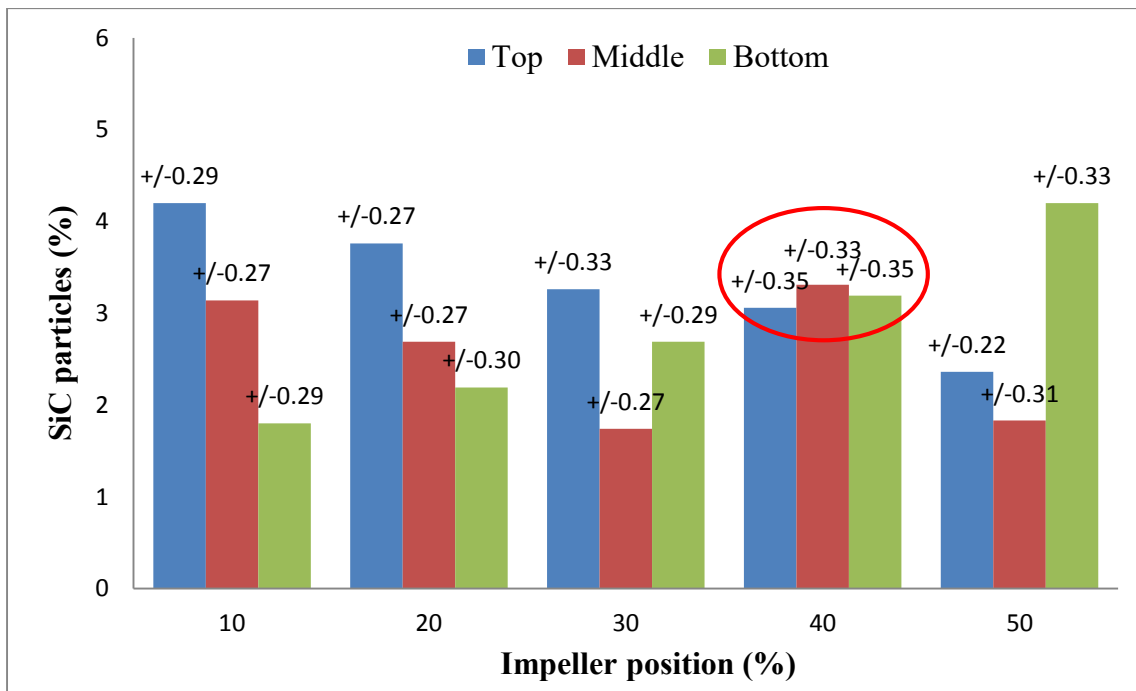


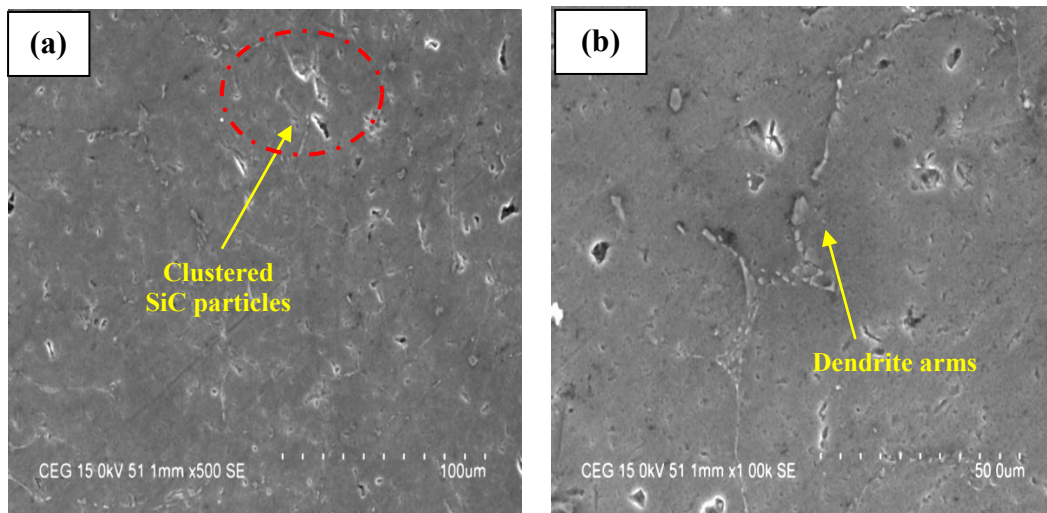
Fig. 10. Percentage of SiC particles obtained from top, middle and bottom of the container with respect to various impeller positions.

3.4 Confirmation experiments

Confirmation experiments were carried out with three different viscosities of the Al melt. Al8011 alloy was selected as the matrix material and SiC particles with 63 microns were chosen as the reinforcement. Chemical composition (wt. %) of Aluminium 8011 studied in this research is formed from Silicon - 0.213, Iron - 0.40, Copper - 0.10, Manganese - 0.018, Magnesium-0.10, Titanium-0.009, Zinc-0.210, Lead-0.009, Tin-0.030, Bismuth-0.002, Zirconium-0.002, chromium-0.002 and remaining Aluminium - 98.905. During the processing of the Al-SiC composite, the SiC particle was preheated in an electric oven to 350 °C. After the complete melting of aluminum billet, the reinforcing material was introduced into the molten metal through the particle injection chamber during the stirring operation. The reason for the preheating of the SiC particle was to improve the sufficient wettability of the matrix and the reinforcement; in turn they prevent the agglomeration of the SiC particles. The stirring was continued for 10min. Finally, the molten metal was poured into the die for getting the cast sample. Three samples were fabricated, sample 1 with 1.24, sample 2 with 1.13 and sample 3 with 1.04 mPa.s viscosity of Al melt by considering all the parameters (45° blade angle, 40% impeller position and 250 rpm stirring speed) as constants. In order to prove the results from the glycerol–water based experiments, microstructural analysis and mechanical testing were carried out.

3.4.1 Microstructural analysis

From the microstructural evaluation (Fig. 11), it was obtained that the 1.24mPa.s viscosity of Al melt possesses more clustering and void formation [22]. Such viscosity of Al represents the 700 °C of working temperature, so at that viscosity, the distribution of the reinforcement was difficult as the particles were resisted by the viscous nature of the fluid but at 1.04mPa.s some voids were formed. This was due to the bubble formation and air entrapment during the stirring, which occurred at the lower viscosity of Al melts (800 °C). It was evident in Fig. 11 that the viscosity of 1.13mPa.s shows enhanced distribution of the reinforcement particles. This represents the working temperature of 750 °C is optimum for the uniform distribution of the particles.



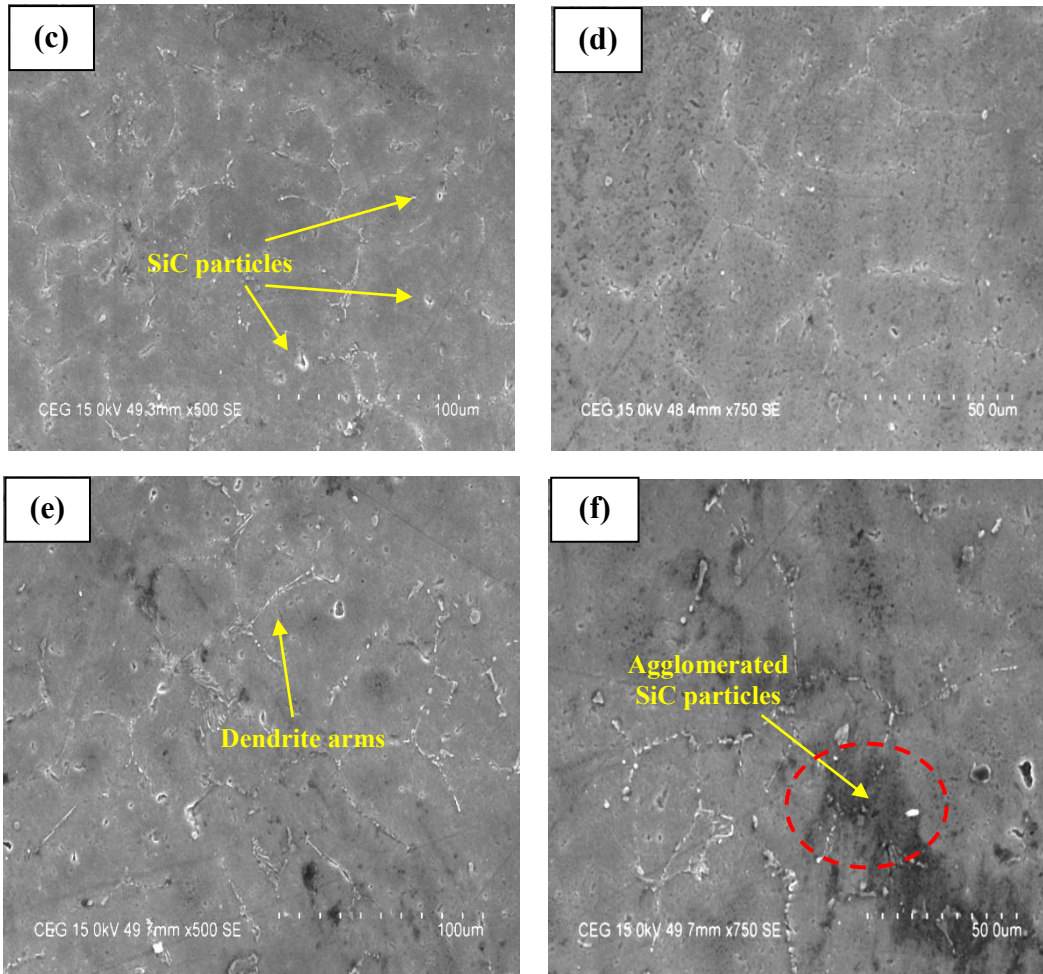


Fig. 11. SEM images of samples at: (a, b) 1.24 mPa.s, (c, d) 1.13 mPa.s and (e, f) 1.04 mPa.s.

3.4.2 Tensile strength

The specimens for tensile testing were cut as per ASTM E-8 standard using Wire cut Electric Discharge Machining (WEDM). Then, the tensile test trials were carried out using universal testing machine. Five specimens were tested for each sample and the averages were presented here. From the tensile test results (Fig. 12), a low value of 64.55 MPa was obtained for the composite prepared with 1.24 mPa.s viscosity of Al melt, due to the inhomogeneity of the reinforcement particles. The tensile strength value of the composite processed at 1.04 mPa.s viscosity of the Al melt was also low when compared to the composite processed at 1.13 mPa.s viscosity of the Al. It is clear that the void formation decreases the tensile strength [23]. Brittle fracture plays a superior role in the composite processed at 1.24 mPa.s viscosity of Al melt (Figs. 13(a) and (b)) and ductile fracture plays an inferior role in the composite processed at 1.04 mPa.s viscosity of Al melt (Figs. 13(e) and (f)). After the application of load, the crack initiated and propagated throughout the agglomerated region of casted samples because of the improper distribution of the SiC particles. This was the reason behind the brittle fracture at the composite processed at 1.24 mPa.s viscosity of Al melt. Similarly, due to the void formation and improper distribution of SiC particles in the composite processed at 1.04 mPa.s viscosity of Al melt, the crack propagate through the voids that are present in the casted samples and also we suspect that in most of the material can occur a lack of SiC particles which led to the ductile behaviour of the casted samples. A mixture of ductile

and brittle fracture was observed in Figs. 13(c) and (d), which proves the uniform distribution of the reinforcement particles.

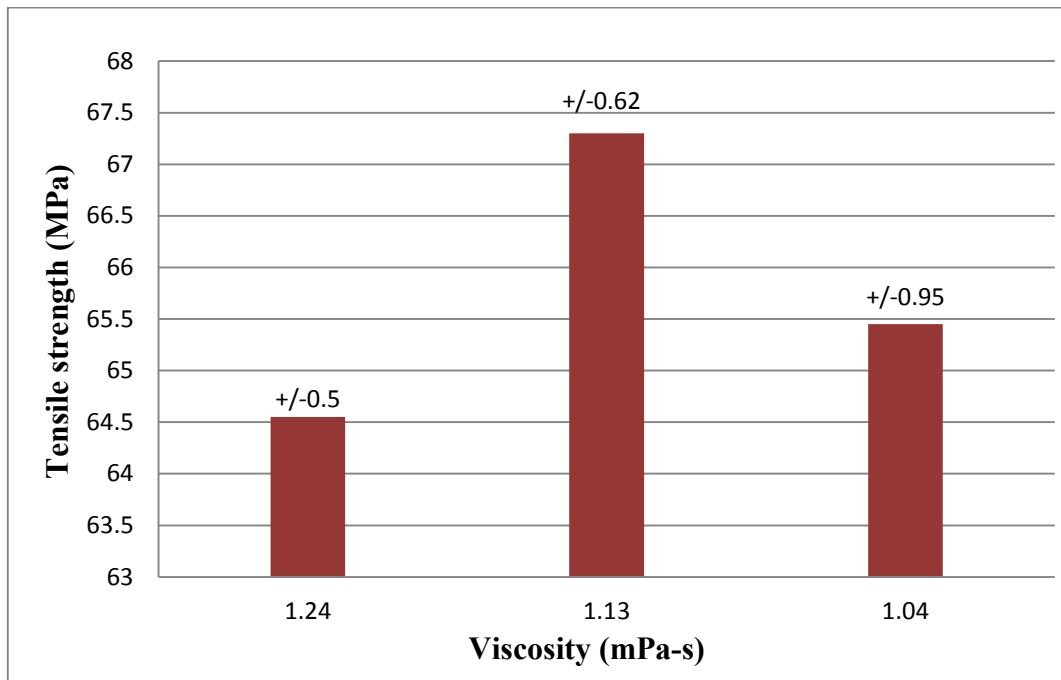
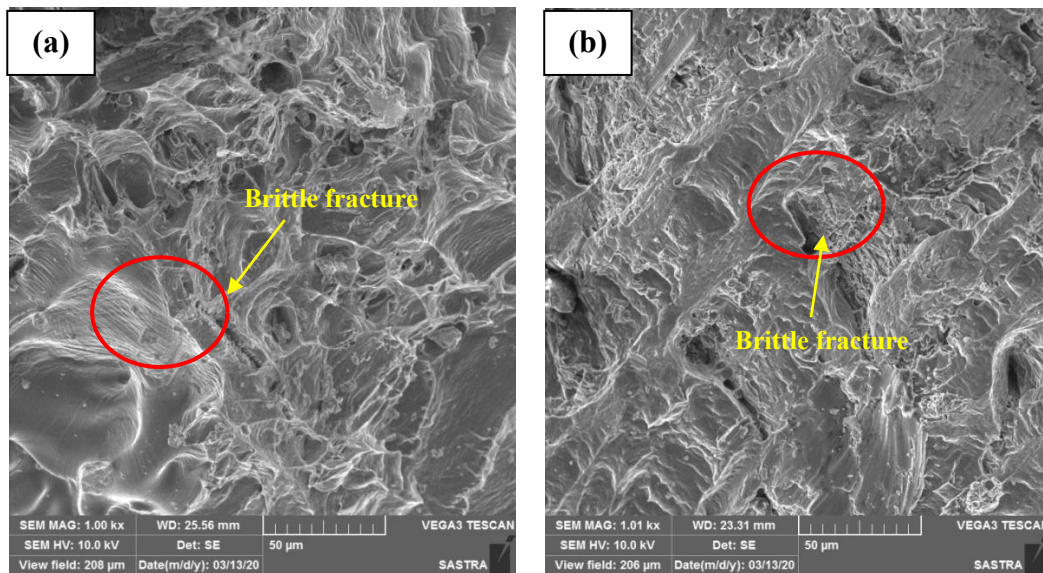


Fig. 12. Tensile strength vs. viscosity.



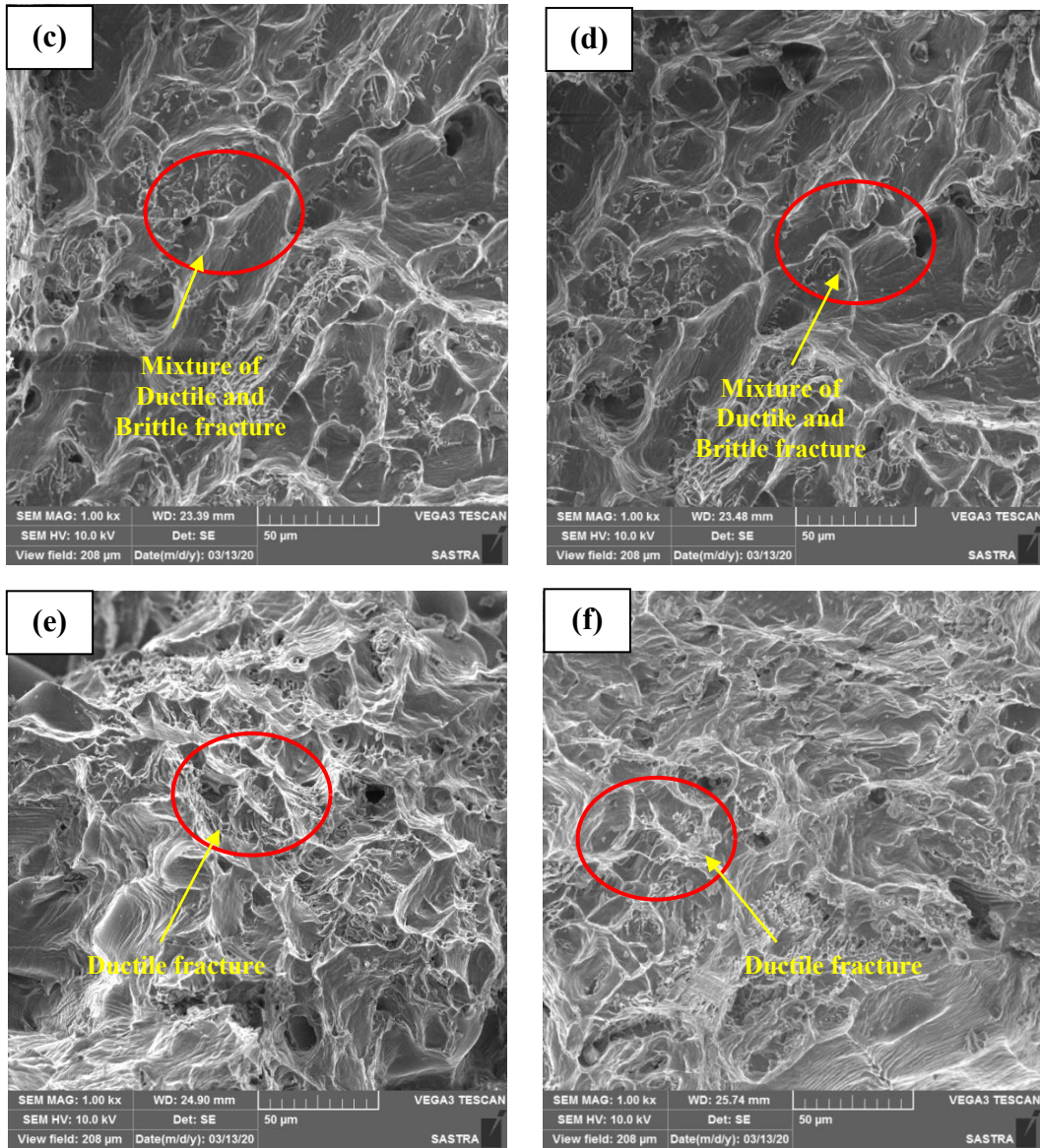


Fig. 13. SEM images of the fractured surfaces of the samples: (a,b) 1.24 mPa.s, (c,d) 1.13 mPa.s, and (e,f) 1.04 mPa.s.

3.4.3 Vickers hardness

The specimens for Vickers hardness test were cut as per ASTM E-92 standard. Vickers hardness test was performed on the samples at the equal interval distance of 6 mm from one end (Figs .14 (a) and (b)). For each sample, six indentations were taken from the various locations of the samples. It was observed that the composite processed at 1.24 mPa.s viscosity of Al melt and the composite processed at 1.04 mPa.s viscosity of Al melt shows significant deviations than the composite processed at 1.13 mPa.s viscosity of Al melt. Such an observation can be related to the presence of voids due to air entrapment and agglomeration of the reinforcement particles [24]. These kinds of variation in the hardness values were due to the improper distribution of the SiC particles. Higher harness values are obtained from the region of higher concentration of SiC particles whereas lower hardness values were obtained in the region of lower concentration of SiC particles. The hardness values of the composite

processed at 1.13 mPa.s viscosity of Al melt were more or less unchanged throughout the composite, which proves that the composite processed at 1.13 mPa.s viscosity of Al melt possess uniform distribution of the reinforcement particles.

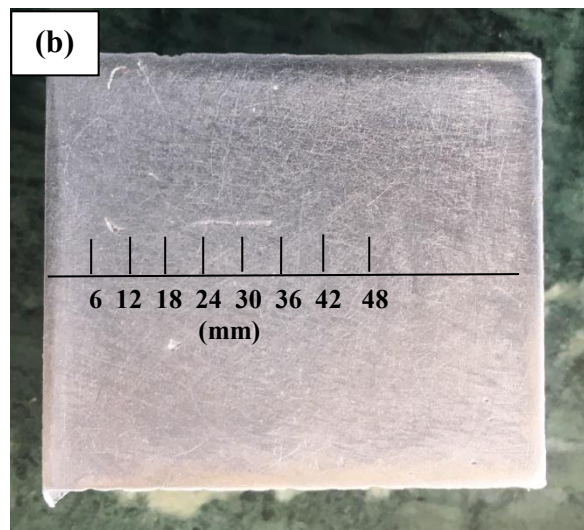
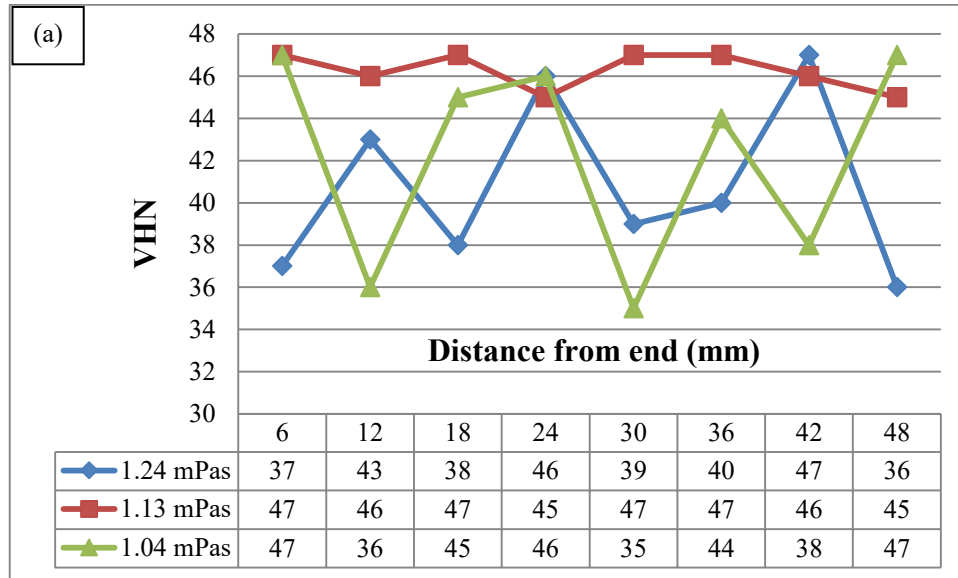


Fig. 14.(a) Hardness vs. distance from one end and (b) schematic representation of distances.

3.4.4 Wear performance

Wear testing was conducted using the pin-on-disc wear testing apparatus (TR-20LE, DUCOM). The test specimens of 6mm diameter and 25mm length were prepared by machining [25]. The trials conducted on the dry sliding condition as accordingly to ASTM G-99 standard. As the load was applied over the pin, the composite pin began to slide over the counter face disc and wear debris were formed. These wear debris acted as a third body abrasion and grooves were formed by ploughing action. Wear rate was evaluated for 1000, 1250 and 1500m sliding distance. Worn-out surfaces of the samples are shown in the Fig. 15. The results revealed that the composite processed at 1.13 mPa.s viscosity of Al melt shows less wear rate than the other samples (Fig. 16). The composite processed at 1.24 mPa.s

viscosity of Al melt shows high wear rate due to the presence of clustering of the SiC particles. Similarly, the composite processed at 1.04 mPa.s viscosity of Al melt also shows high wear rate due to the void formation and improper distribution. The main reason for the higher wear rate was due to the clustering and the agglomeration of SiC particles. Here, the term clustering refers to the bunch or group of SiC particles that are close to each other, and agglomeration refers to the collection of SiC particles forming a mass or heap. It can be concluded that the composite processed at 1.13 mPa.s viscosity of Al melt with uniform distribution of the SiC particles showed a better wear performance.

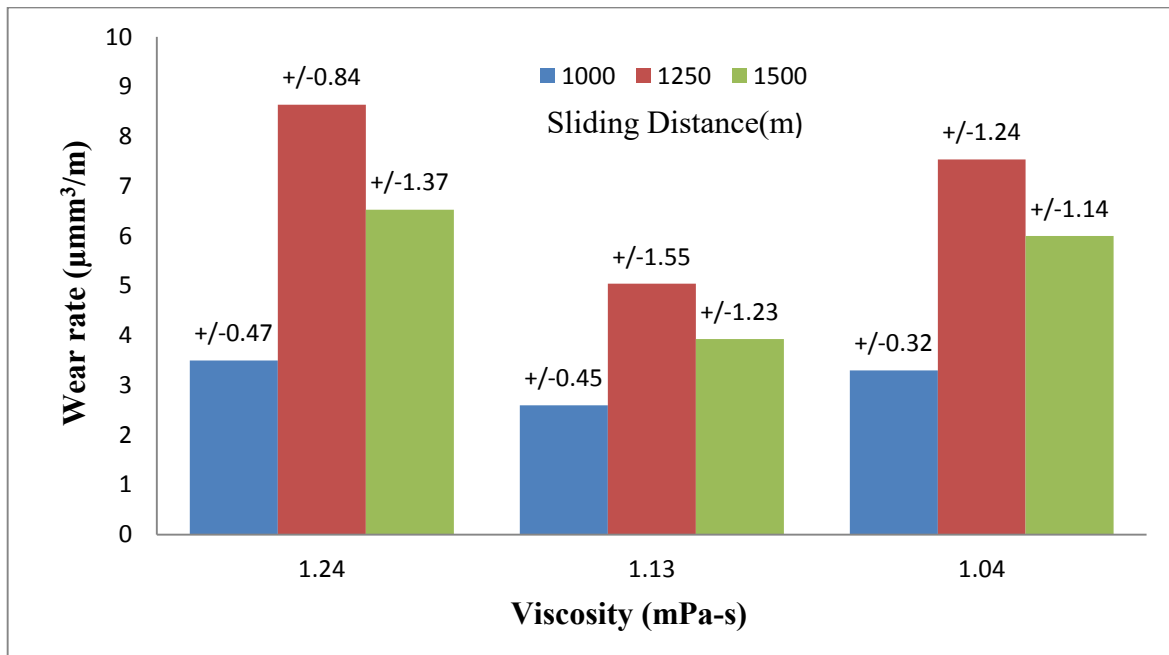
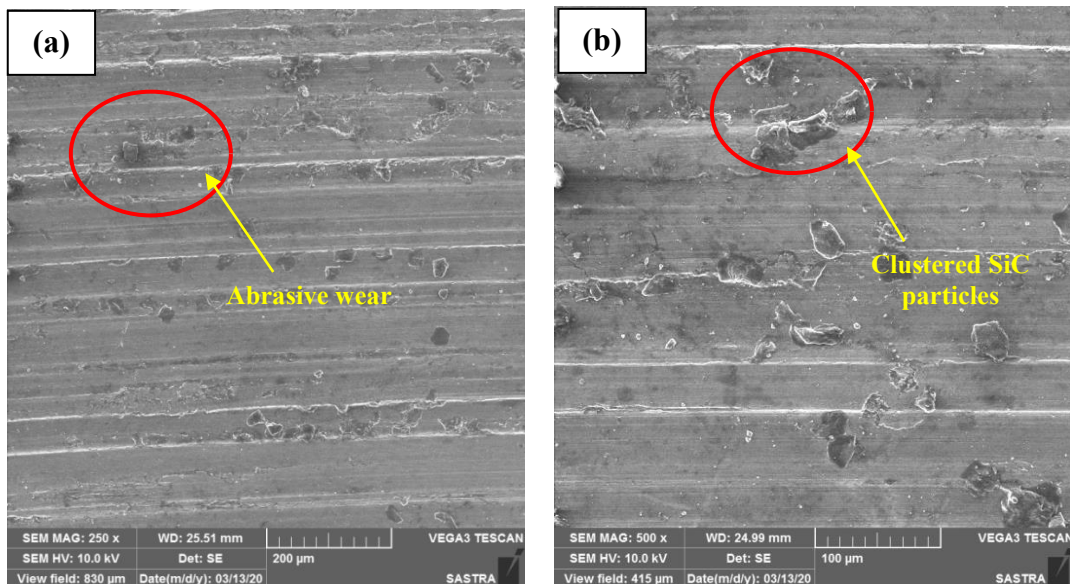


Fig.15. Wear rate vs.viscosity.



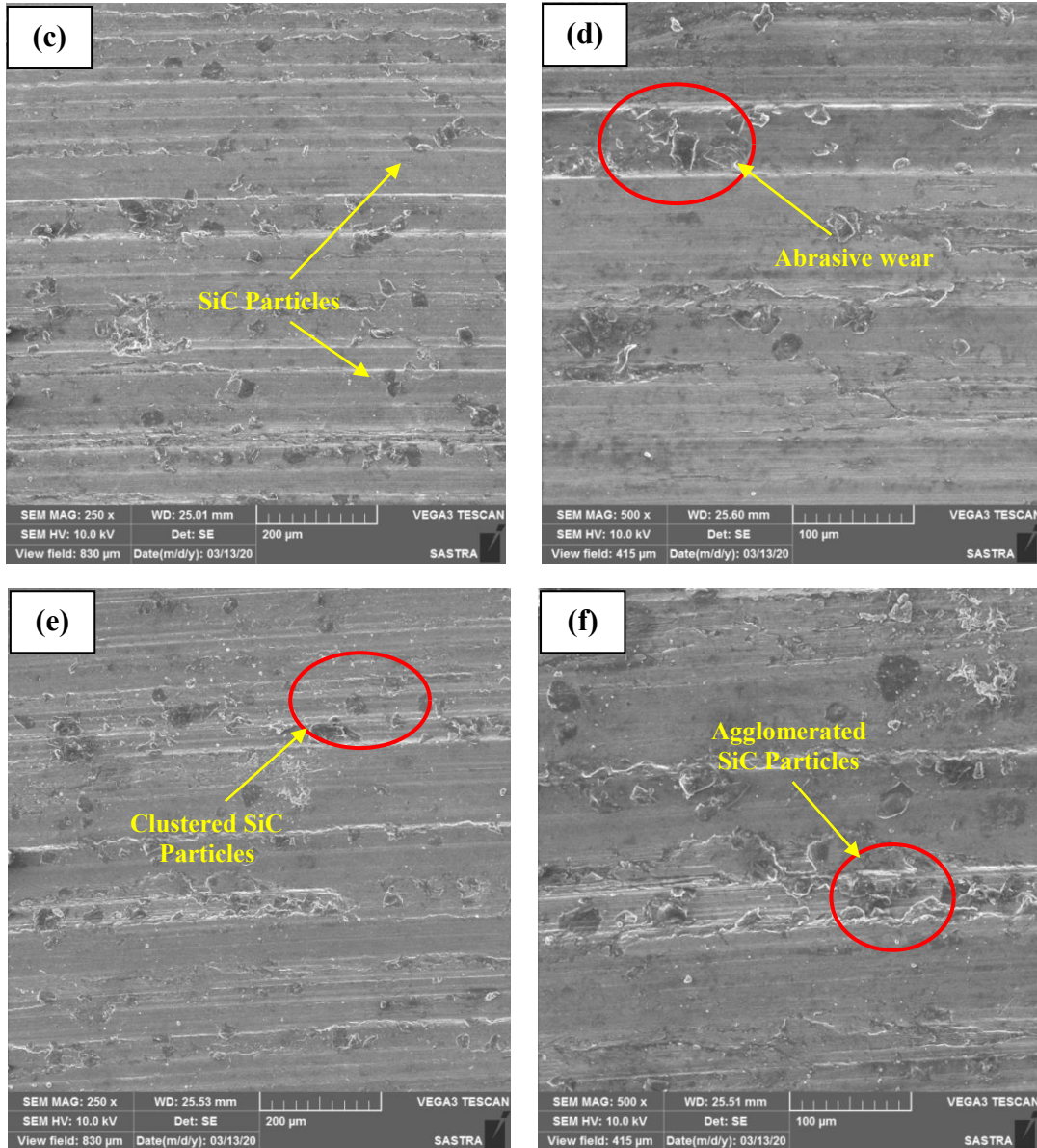


Fig. 16. SEM images of the worn surfaces of the samples: (a, b) 1.24mPa.s, (c, d) 1.13mPa.sand (e, f) 1.04mPa.s.

4. Conclusions

Experimental investigations were carried out using glycerol–water based model. The findings of the investigations were validated by confirmation experiments. The outcome of the confirmation experiments showed that the uniform distribution of the reinforcement particles led to significant improvement in overall strength of the composites. The following conclusions were drawn from the investigations:

- 1.13mPa.s viscosity of Al melt eliminated agglomeration and void formation which showed enhanced distribution of the particles leading to the improvement of tensile strength by 4%, wear resistance by 21% and uniform hardness of 47 VHN throughout the composites.

- The optimum dispersion time of the reinforcement particles was 15 seconds which was obtained by 45° blade angle and 250 rpm stirring.
- The bubble formation and the air entrapment were prevented by the optimum vortex height of 6 mm provided by stirrer height at 40% from the bottom and 1.13mPa.s viscosity of Al melt.

References

- 1) Rohatgi, P. K., Ray, S., Asthana, R., & Narendranath, C. S. (1993). Interfaces in cast metal-matrix composites. *Materials Science and Engineering: A*, 162(1-2), 163-174.
- 2) Miani, F., & Matteazzi, P. (1992). Estimation of viscosity in undercooled liquid metal alloys. *Journal of non-crystalline solids*, 143, 140-146.
- 3) Wang, J., Guo, Q., Nishio, M., Ogawa, H., Shu, D., Li, K., ...& Sun, B. (2003). The apparent viscosity of fine particle reinforced composite melt. *Journal of materials processing technology*, 136(1-3), 60-63.
- 4) Huang, S. J., & Abbas, A. (2020). Effects of tungsten disulfide on microstructure and mechanical properties of AZ91 magnesium alloy manufactured by stir casting. *Journal of Alloys and Compounds*, 817, 153321.
- 5) Venkatesh, C., & Venkatesan, R. (2015). Optimization of process parameters of hot extrusion of SiC/Al 6061 composite using Taguchi's technique and upper bound technique. *Materials and Manufacturing Processes*, 30(1), 85-92.
- 6) Akinwamide, S. O., Abe, B. T., Akinribide, O. J., Obadele, B. A., & Olubambi, P. A. (2020). Characterization of microstructure, mechanical properties and corrosion response of aluminium-based composites fabricated via casting—a review. *The International Journal of Advanced Manufacturing Technology*, 1-17.
- 7) Kumar, A., Pal, K., & Mula, S. (2021). Effects of cryo-FSP on metallurgical and mechanical properties of stir cast Al7075–SiC nanocomposites. *Journal of Alloys and Compounds*, 852, 156925.
- 8) Dey, D., & Biswas, A. (2020). Comparative Study of Physical, Mechanical and Tribological Properties of Al2024 Alloy and SiC-TiB 2 Composites. *Silicon*, 1-12.
- 9) Sahu, M. K., & Sahu, R. K. (2017). Optimization of stirring parameters using CFD simulations for HAMCs Synthesis by stir casting process. *Transactions of the Indian Institute of Metals*, 70(10), 2563-2570.

- 10) Zhang, P., Zhang, W., Du, Y., & Wang, Y. (2020). High-performance Al-1.5 wt% Si-Al₂O₃ composite by vortex-free high-speed stir casting. *Journal of Manufacturing Processes*, 56, 1126-1135.
- 11) Nageswaran, G., Natarajan, S., & Ramkumar, K. R. (2018). Synthesis, structural characterization, mechanical and wear behaviour of Cu-TiO₂-Gr hybrid composite through stir casting technique. *Journal of Alloys and Compounds*, 768, 733-741.
- 12) Gupta, M. K., Gangil, B., & Ranakoti, L. (2020). Mechanical and Tribological Characterizations of Al/TiB₂ composites. *Industrial Engineering Journal*, 13(4).
- 13) Lee, D., Kim, J., Lee, S. K., Kim, Y., Lee, S. B., & Cho, S. (2020). Experimental and thermodynamic study on interfacial reaction of B₄C-Al6061 composites fabricated by stir casting process. *Journal of Alloys and Compounds*, 157813.
- 14) Sharma, A., Rastogi, V., & Agrawal, A. K. (2020). Multi-Parametric Optimisation by Quantitative Assessment of Distribution Index and Area Fraction of Composite. *Practical Metallography*, 57(9), 588-613.
- 15) Nanjan, S., & Murali, J. G. (2020). Analysing the Mechanical Properties and Corrosion Phenomenon of Reinforced Metal Matrix Composite. *Materials Research*, 23(2).
- 16) Zhang, W. Y., Du, Y. H., & Zhang, P. (2019). Vortex-free stir casting of Al-1.5 wt% Si-SiC composite. *Journal of Alloys and Compounds*, 787, 206-215.
- 17) Sahu, M. K., Valarmathi, A., Baskaran, S., Anandakrishnan, V., & Pandey, R. K. (2014) Multi-objective optimization of upsetting parameters of Al-TiC metal matrix composites: A grey Taguchi approach. *Proceedings of the Institution of Mechanical Engineers, Part B: Journal of Engineering Manufacture*, 228(11), 1501-1507.
- 18) Dutta, Sunil, and Suresh Kumar Reddy Narala (2020). Experimental investigation to study the effects of processing parameters on developed novel AM (Al-Mn) series alloy. *Materials and Manufacturing Processes*, 1-10.
- 19) Kumar, A., Kumar, P., & Singh, R. C. (2020). The effect of alumina on mechanical behavior of Al 6064 alloy. In *IOP Conference Series: Materials Science and Engineering*, Vol. 802, No. 1, p. 012004.
- 20) Kumar, S., & Vasumathi, M. (2020). Applying visualization techniques to study the fluid flow pattern and the particle distribution in the casting of metal matrix composites. *Journal of Manufacturing Processes*, 58, 668-676.
- 21) M. Saravanakumar., Begum, S. R., & Vasumathi, M. (2019) Influence of stir casting parameters on particle distribution in metal matrix composites using stir casting process. *Materials Research Express*, 6(10), 1065d4.
- 22) Zhang, W. Y., Du, Y. H., & Zhang, P. (2019). Vortex-free stir casting of Al-1.5 wt% Si-SiC composite. *Journal of Alloys and Compounds*, 787, 206-215.

- 1
2
3
4
5
6
7
8
9
10
11
12
13
14
15
16
17
18
19
20
21
22
23
24
25
26
27
28
29
30
31
32
33
34
35
36
37
38
39
40
41
42
43
44
45
46
47
48
49
50
51
52
53
54
55
56
57
58
59
60
61
62
63
64
65
- 23) Shayan, M., Eghbali, B., & Niroumand, B. (2020). The role of accumulative roll bonding after stir casting process to fabricate high-strength and nanostructured AA2024-(SiO₂+ TiO₂) hybrid nanocomposite. *Journal of Alloys and Compounds*, 845, 156281.
- 24) Krishnan, P. K., Christy, J. V., Arunachalam, R., Mourad, A. H. I., Muraliraja, R., Al-Maharbi, M., ... & Chandra, M. M. (2019). Production of aluminum alloy-based metal matrix composites using scrap aluminum alloy and waste materials: Influence on microstructure and mechanical properties. *Journal of Alloys and Compounds*, 784, 1047-1061.
- 25) Kumar, M. S., Pruncu, C. I., Harikrishnan, P., Begum, S. R., & Vasumathi, M. (2021). Experimental investigation of in-homogeneity in particle distribution during the processing of metal matrix composites. *Silicon*, 1-13.